SubCALM: A Program for Hierarchical Substrate Coupling Simulation on Floorplan Level

Thomas Brandtner
Infineon Technologies
Development Center Villach, Austria
thomas.brandtner@infineon.com

Robert Weigel
Chair of Electronics
University of Erlangen-Nuremberg, Germany
weigel@lte.e-technik.uni-erlangen.de

Abstract

The hierarchical substrate coupling simulation tool SubCALM offers the opportunity to estimate substrate coupling on floorplan level. A novel approach for modeling well and SOI structures in a boundary element description is introduced. Several acceleration techniques like precalculated macromodels and sophisticated preconditioning algorithms are presented which are applied to an O(n)-conjugate-gradient Poisson solver in order to be able to process large full-chip layouts during floorplanning.

1. Introduction

Due to the ongoing trend to higher integration modern mixed-signal IC designs consist of an increasing number of analogue and digital subcircuits. This enables digital interference to couple to sensitive analogue nodes through the substrate [1]. Most of the substrate noise on chip level is coupled via low-ohmic substrate contacts and the power supply network [2]. Therefore, the positive or even negative influence of substrate coupling countermeasures like spatial separation or guard rings [3] can be estimated accurately only on floorplan level since their efficiency heavily depends on the impedance of the global power supply network. Unfortunately, traditional substrate coupling simulation tools [4] do not offer this opportunity since they do not provide the possibility to carry out a complete co-simulation of substrate coupling together with the power supply grid. Furthermore, they perform a substrate impedance extraction based on a flattened layout, which is not feasible for large full-chip layouts.

Having all this in mind, a substrate coupling estimation tool named SUBCALM has been developed. The basic approach and several measurement results for verification in $0.13\,\mu$m CMOS and $0.25\,\mu$m BiCMOS technologies have been published in [5, 6]. The tool exploits the boundary element method (BEM) and contains a Poisson solver based on an O(n) conjugate gradient algorithm [7]. In addition, it offers the opportunity to consider the influence of the impedance of the power supply network defined by a SPICE netlist [5]. In Sect. 2 an enhancement of the basic algorithm is presented that now even supports the simulation of noise coupling from metal lines into the substrate (Fig. 1). Section 3 introduces a novel approach in order to model well and SOI structures, which is usually not possible with BEM. It turned out that all these measures are still not sufficient to provide a software tool which is able to process large mixed-signal designs on floorplan level. Hence precalculated macromodels and preconditioning algorithms are presented in Sect. 4. Macromodels offer different user-defined abstraction levels and are well suited to a hierarchical design flow. Finally an application of SUBCALM with its new hierarchical design flow for substrate coupling estimation is demonstrated.

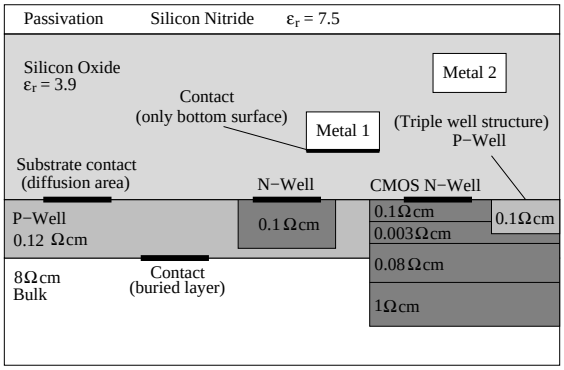

Figure 1. Simplified layer structure of a BiCMOS technology.

2. Combined substrate and oxide layer model

The substrate of an IC fabricated in a CMOS, BiCMOS or bipolar technology may be modeled as a semi-infinite halfspace of silicon with different layers of resistivity depending on the doping density. This simplified model and its mathematical treatment have been presented in [5]. How-

1530-1591/04 $20.00 (c) 2004 IEEE

ever, this model can be extended to oxide layers, which makes it possible to define non-conducting layers like SOI layers inside the bulk. Moreover, oxide layers on top of the substrate may be defined as well. This offers the opportunity to simulate noise coupling between metal layers and the substrate which becomes more and more important as pointed out in [8]. Let Ω be the domain of the problem that comprises conductive layers with conductivity σ and insulating layers with permittivity ε as shown in Fig. 1. Domain Ω is connected to external electrical nets either via highly doped diffusion areas and buried layers, or by the surface of metal lines located in the oxide area.

One major simplification is made by the assumption that every contact is infinitely thin and always perpendicular to the z-axis. This is sufficient for substrate coupling analysis, since diffusion and buried layer structures are always thin in comparison with the thickness of substrate layers. Furthermore, it is valid to define only a contact at the bottom surface of each metal line as far as coupling to the substrate is concerned. However, it is planned to improve SUBCALM such that it will be able to model side wall and top surface contacts as well. With this extension SUBCALM may be also used to calculate the capacitance between different metal lines as in this case side walls must not be neglected. Traditional capacitance extraction tools consider only the pure capacitive coupling, SUBCALM will also include additional coupling paths through the substrate. This application in parasitic capacitance calculation is justified since SUBCALM exploits algorithms that are successfully used in capacitance extraction [9, 10].

A presentation of a simplified model for substrate coupling simulation has been given in [5] based on the assumption that the substrate consists of different conductive layers with conductivity σ. This approach can be extended to non-conductive oxide layers by introducing a generalized complex conductivity

$$\kappa = \sigma + j\omega\varepsilon \tag{1}$$

This leads to a quasi-electrostatic current flow problem between certain contacts that is expressed mathematically by the Poisson equation

$$\Delta\phi(\vec{r}) = -\frac{1}{\kappa(\vec{r})} J(\vec{r}) \tag{2}$$

where $\phi(\vec{r})$ is the scalar potential at point $\vec{r}$ in Ω due to injected currents with current density $J(\vec{r})$. SUBCALM exploits the boundary element method (BEM) and Galerkin's approach to solve (2) numerically. Each contact is subdivided into smaller rectangles assuming constant potential and constant current density across such a rectangle. This results in a dense linear system

$$\mathbf{Zi} = \mathbf{v} \tag{3}$$

with an impedance matrix $\mathbf{Z}$, a vector $\mathbf{i}$ containing all injected currents and a vector $\mathbf{v}$ defining the potentials of all contacts. Each entry of $\mathbf{Z}$ is determined by integrating the appropriate Green's function G over the surface of each rectangle. The Green's function has to satisfy

$$\nabla\left[G(\vec{r},\vec{r}_0)\right] = -\frac{\delta(\vec{r}-\vec{r}_0)}{\kappa(\vec{r})} \tag{4}$$

and may be determined by an algorithm based on the Fast-Hankel-Transform similar to the one presented in [5], but with σ replaced by κ. Several different algorithms have been proposed in literature to solve (3) in subquadratic time. Most of them are based on multipole expansion with $O(n)$ time consumption like FastCap [9]. SUBCALM exploits the hierarchical algorithm of Appel [7, 10] with a linear time complexity. This basic algorithm has been enhanced in order to cope with well structures and huge layouts as presented in the next sections.

3. Simulation of well structures

Well structures cannot be simulated by the BEM algorithm easily since it is only possible to model layer structures that change in z-direction, because radial invariance has been assumed for the derivation of the Green's function. However, it will be shown in this section that the calculation of the impedance matrix $\mathbf{Z}$ can be modified in order to process even triple well structures. A simplified well structure is shown in Fig. 2. The pn-junction at the interface between wells is replaced by special 'well contacts'. The current I_w flows through such a contact. Since the pn-junction is reversely biased, its junction capacitance C_j has to be added to the model:

$$C_\mathrm{j} = C_\mathrm{j0}\left(1 + \frac{V_\mathrm{w} - V'_\mathrm{w}}{V_\mathrm{j}}\right)^{-M} \tag{5}$$

Two different potentials V_w and V'_w are dedicated to each well contact depending from which side it is looked at. C_j0, V_j and M are parameters of the commonly used SPICE model for the junction capacitance. They are usually determined by measurement. In most cases a well structure is large with respect to the thickness of substrate contacts and wells, which are typical only a few μm in depth. Hence it is possible to neglect all the side walls of the wells, at least since SUBCALM is meant to be used primarily for substrate coupling simulation on floorplan level. For exact simulations on particular small substrate structures FEM based simulators like [4] are a better choice. However, it is planned to implement the capability to treat even side wall capacitances into a future version of SUBCALM.

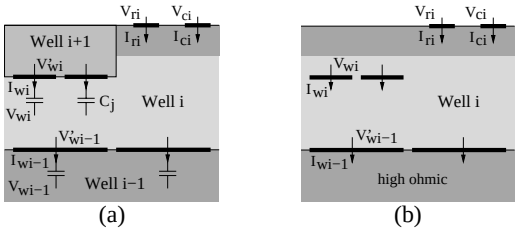

Figure 2. Modeling of wells in SUBCALM.

Considering only well i, all subwells $i+1$ are removed first. In addition, a high ohmic layer is introduced instead of parent well $i-1$ as shown in Fig. 2b. For each well a complete set of Green's functions is determined first. An impedance matrix $\mathbf{Z}'_{well}$ of this modified structure is calculated.

$$\begin{pmatrix} V'_{\mathrm{w},i-1} \\ V_{\mathrm{r},i} \\ V_{\mathrm{c},i} \\ V_{\mathrm{w},i} \end{pmatrix} = \begin{pmatrix} Z'_{11} & Z'_{12} & Z'_{13} & Z'_{14} \\ Z'_{21} & Z'_{22} & Z'_{23} & Z'_{24} \\ Z'_{31} & Z'_{32} & Z'_{33} & Z'_{34} \\ Z'_{41} & Z'_{42} & Z'_{43} & Z'_{44} \end{pmatrix} \begin{pmatrix} -I_{\mathrm{w},i-1} \\ I_{\mathrm{r},i} \\ I_{\mathrm{c},i} \\ I_{\mathrm{w},i} \end{pmatrix} \quad (6)$$

where $I_{\mathrm{c},i}$ and $V_{\mathrm{c},i}$ denote currents resp. voltages which are dedicated to substrate contacts or metal lines located in or over well i. One arbitrary contact within each well i is chosen to be the reference contact. Since a well is a closed volume,

$$I_{r,i} = I_{w,i-1} - I_{c,i} - I_{w,i} \quad (7)$$

has to hold. Hence $\mathbf{Z}'_{\mathbf{well}}$ is over-determined. The variables dedicated to the reference contact $I_{\mathrm{r},i}$ and $V_{\mathrm{r},i}$ are removed leading to $\mathbf{Z_{well}}$ with entries $Z_{\mathrm{well},jk}$. The influence of the junction capacitances can be considered as follows.

$$V_{\mathrm{w},i-1} = V'_{\mathrm{w},i-1} - \frac{1}{j\omega C_{\mathrm{j}}} I_{\mathrm{w},i-1} \quad (8)$$

This results in an impedance matrix $\mathbf{Z}_{\mathbf{well},i}$ for every well.

$$\begin{pmatrix} V_{\mathrm{w},i-1} - V_{\mathrm{r},i} \\ V_{\mathrm{c},i} - V_{\mathrm{r},i} \\ V_{\mathrm{w},i} - V_{\mathrm{r},i} \end{pmatrix} = \begin{pmatrix} Z_{\mathrm{well},11} + \mathrm{diag}\frac{1}{j\omega C_{\mathrm{j}}} \cdots \\ Z_{\mathrm{well},21} \quad \ddots \\ Z_{\mathrm{well},31} \quad \cdots \end{pmatrix} \begin{pmatrix} -I_{\mathrm{w},i-1} \\ I_{\mathrm{c},i} \\ I_{\mathrm{w},i} \end{pmatrix} \quad (9)$$

All these matrices can be summed up in a symmetric impedance matrix $\mathbf{Z}$ for the whole system.

$$\begin{pmatrix} V_{\mathrm{c},0} - V_{\mathrm{r},0} \\ V_{\mathrm{r},1} - V_{\mathrm{r},0} \\ -(V_{\mathrm{c},1} - V_{\mathrm{r},1}) \\ -(V_{\mathrm{r},2} - V_{\mathrm{r},1}) \\ V_{\mathrm{c},2} - V_{\mathrm{r},2} \end{pmatrix} = \begin{pmatrix} \mathbf{Z_{well,0}} & 0 & 0 & 0 \\ + & & & 0 \\ 0 & \mathbf{Z_{well,1}} & & 0 \\ 0 & & + & \\ 0 & 0 & 0 & \mathbf{Z_{well,2}} \end{pmatrix} \begin{pmatrix} I_{\mathrm{c},0} \\ I_{\mathrm{w},0} \\ -I_{\mathrm{c},1} \\ -I_{\mathrm{w},1} \\ I_{\mathrm{c},2} \end{pmatrix} \quad (10)$$

The above approach can be easily extended to more contacts per well. All entries in $\mathbf{Z}'_{\mathbf{well}}$ and $\mathbf{Z_{well}}$ except those for reference contacts will convert to submatrices. A modified CG-algorithm [11] has to be used in order to invert the complex symmetric, but not hermitian system impedance matrix $\mathbf{Z}$. The validity of this approach is presented in Fig. 3 by measurement results of well structures on a $0.25\,\mu$m BiCMOS testchip [6]. The influence of the voltage-dependent pn-junction capacitance between the well and the bulk may be easily seen. The difference between measurement and simulation is less than 5 dB, which is sufficient for a coupling estimation. At frequencies above several GHz coupling from the well into the substrate becomes as strong as pure substrate coupling without any well structure. Hence the possibility to simulate the influence of wells is an essential feature for simulation tools used to examine the RF behaviour of the substrate.

The algorithm of this section can also be used to model SOI technologies. In such a case the layer structure contains a thin insulating layer. The according Green's function can be calculated as mentioned in Sect. 2. Subsequently, virtual 'SOI contacts' are defined for each SOI region. The regions are insulated from each other by trenches (Fig. 4). An impedance matrix $\mathbf{Z_{SOI},}_i$ for every SOI region can be calculation quite similar to (9), but without the additional diag-term with the junction capacitance. Again, direct coupling between two SOI regions is neglected, which is an restriction of the current version of SUBCALM.

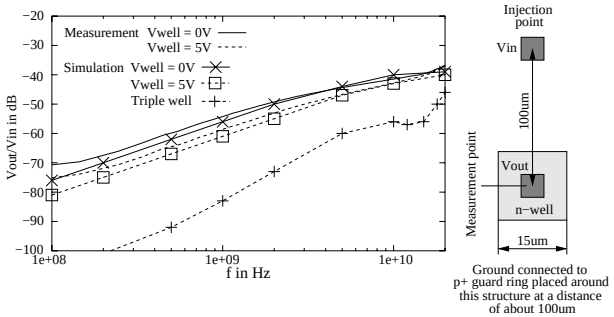

Figure 3. Measurement and simulation results of a BiCMOS triple well structure.

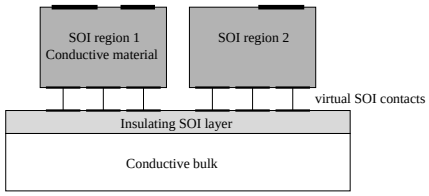

Figure 4. SOI extension of BEM algorithm.

4. Acceleration of calculation

The most time consuming part of BEM-based substrate coupling simulation is the inversion of $\mathbf{Z}$. Although an O(n)-CG-Poisson solver is implemented in SUBCALM, further measures have to be taken in order to make simulation on floorplan level computational feasible or even possible.

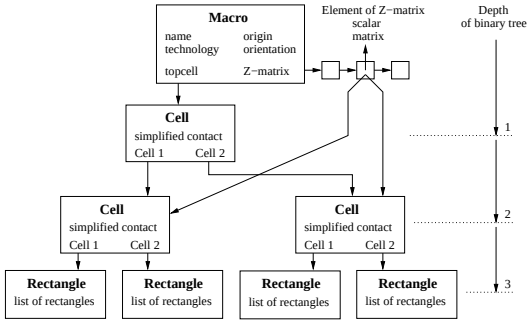

Figure 5. Internal layout and coupling representation.

4.1. Precalculated macromodels

The accelerated CG-algorithm of SUBCALM exploits the smooth decrease of the modified Green's function. Hence coupling coefficients Z_{ij} and Z_{ik} of three contacts i, j and k are almost equal, if j and k are located far away from i [6]. Hence it is sufficient to take only the monopole term of the multipole expansion of the superposition of the electrostatic coupling originated by contacts i and j. The geometric description of all contacts is stored in a binary tree (Fig. 5).

The toplevel layout is represented by the macro object. The contacts are subdivided into smaller rectangles. Adjacent rectangles are stored in rectangle objects that form the leaves of the tree. Cell objects act as internal branches. In addition, a cell object combines all rectangles of its child nodes to one big simplified circular substrate contact which represents the monopole term of all rectangles located in its child nodes. The coupling coefficients Z_{ij} are entries of a single linked list. Each list element contains pointers to two nodes of the tree and the dedicated coupling data. This data may be a submatrix of $\mathbf{Z}$, if both pointers point to rectangle objects which store rectangles that are not far separated. On the other hand, the data entry may represent the coupling coefficient between two simplified circular contacts located far away from each other. One constraint of this approach is the fact that the whole layout is stored inside the binary tree. Hence every rectangle is linked to a variable leading to several 100000 variables in total for a full-chip simulation. Precalculated macromodels solve this problem.

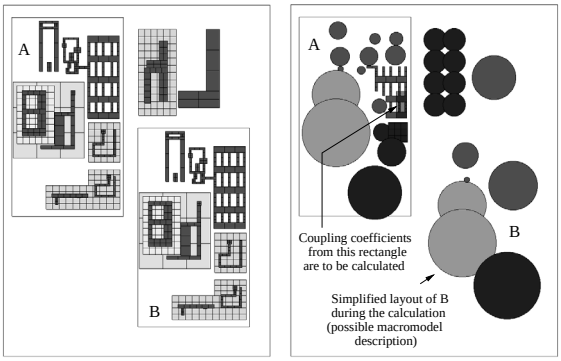

Figure 6. Example layout with two subcircuits and their simplification during calculation.

A simple layout with two subcircuits A and B and the approximation algorithm is visualized in Fig. 6. If the coupling coefficients between a certain rectangle R_A in A and all the other layout objects are considered only, it becomes obvious that it is not necessary to look at the exact layout of subcircuit B, since its rectangles are far away from R_A. However, the exact position of nearby rectangles, which are all part of subcircuit A, is still important. This example shows that it is sufficient to work with simplified versions of the layout of each subcircuit while calculating the coupling coefficients between them. Nevertheless the exact internal structure of a subcircuit must not be simplified, if the coupling coefficients between internal rectangles are determined. A precalculated macromodel is produced as follows. The impedance matrix $\mathbf{Z}$ of the subcircuit is calculated first. Afterwards the binary tree of Fig. 5 is truncated at a certain depth d. All the circular contacts of the cell objects at depth d will act as ports of the new macromodel. The abstraction level may be defined by changing d. Now the admittance matrix $\mathbf{Y_m}$ of the simplified model is determined.

$$\mathbf{Y_m} = \mathbf{P_m}^T \mathbf{Z}^{-1} \mathbf{P_m} \tag{11}$$

where $\mathbf{P_m}$ denotes a projection matrix whose elements $P_{\mathrm{m},ij} = 1$, if rectangle i of the original layout is part of the simplified circular contact j. $\mathbf{Y_m}$ describes the coupling between the new circular ports of the macromodel. Eq. 11 is evaluated by the O(n)-CG-algorithm. Subsequently the impedance matrix of the macro $\mathbf{Z_m} = \mathbf{Y_m}^{-1}$ is determined and stored in a binary file together with the truncated binary tree containing the simplified layout of the precalculated macromodel.

If a layout consisting of two subcircuits like in Fig. 6 should be processed, the precalculated macromodels of both subcircuits A and B with their impedance matrices $\mathbf{Z_{mA}}$ and $\mathbf{Z_{mB}}$ are loaded first. They form the diagonal blocks of the new impedance matrix $\mathbf{Z_{tot}}$. The coupling coefficients between the macros are calculated using the simplified description with circular ports which is a set of monopole sources. Since these ports are located far away from each other, only a small error will occur, because the original O(n)-CG-algorithm would have simplified the coupling coefficients in a similar way. Hence $\mathbf{Z_{tot}} \in C^{k \times k}$, where k denotes the number of macromodel ports of A and B together. It is obvious that k is much smaller than the original number of rectangles. This approach offers the following advantages:

- Smaller equation system, less variables.
- Good estimation of coupling coefficients between the contacts of different subcircuits.
- Exact description of coupling between internal contacts of each subcircuit since the calculation of $\mathbf{Z_m}$ is based on the original exact layout of the subcircuit.

4.2. Preconditioning

The convergence rate of the CG-algorithm depends on the ratio between the maximum and the minimum eigenvalue of $\mathbf{Z}$ [12]. If a $\mathbf{Z}$ with well structures is evaluated for low frequencies, it can become ill-conditioned. Hence the usage of a preconditioner is recommended. This is a common approach in FEM, since efficient preconditioners for sparse matrices exist like, for instance, preconditioners based on incomplete Cholesky decomposition [3]. Unfortunately BEM matrices are dense. However, several different

possibilities for a preconditioning matrix $\mathbf{M}$ were investigated and show quite promising results. In general, $\mathbf{M}$ approximates $\mathbf{Z}$, but is easier to invert. The CG-algorithm is applied to a modified equation system of

$$\mathbf{M}^{-1}\mathbf{Z}\mathbf{i} = \mathbf{M}^{-1}\mathbf{v} \tag{12}$$

The condition number of the modified system matrix is closer to 1, hence the CG-algorithm will converge faster. The following preconditioners are implemented:

- JACOBI (JAC): Only diagonal elements of $\mathbf{Z}$ are considered: $\mathbf{M}^{-1} = \mathrm{diag}(1/Z_{ii})$
- BLOCK JACOBI (BJAC): Coefficients Z_{ij} are considered, if rectangles i and j are located in the same rectangle object. Hence diagonal blocks $\mathbf{Z_k}$ of adjacent entries inside $\mathbf{Z}$ are chosen to form $\mathbf{M_k}^{-1} = \mathrm{diag}(\mathbf{Z_k}^{-1})$, where $\mathbf{M_k}^{-1}$ are diagonal submatrices of $\mathbf{M}^{-1}$.
- OVERLAPPING BLOCK JACOBI (OBJAC): Z_{ij} are stored in a single linked list as mentioned in Sect. 4.1. Some entries contain coupling matrices between two rectangle objects rather than coupling scalars between simplified circular contacts, because the rectangles of these rectangle objects are not that far away. Let $\mathbf{Z}_{k1}$ and $\mathbf{Z}_{k2}$ be the diagonal block matrices for rectangle objects k_1 and k_2, and $\mathbf{Z}_{k1,k2}$ the coupling block matrix between the rectangles of these two objects.

$$\mathbf{M}^{-1}_{k1,k2} = \begin{pmatrix} \mathbf{Y_{11}} & \mathbf{Y_{12}} \\ \mathbf{Y_{12}}^T & \mathbf{Y_{22}} \end{pmatrix} = \begin{pmatrix} \mathbf{Z}_{k1} & \mathbf{Z}_{k1,k2} \\ \mathbf{Z}_{k1,k2}{}^T & \mathbf{Z}_{k2} \end{pmatrix}^{-1} \tag{13}$$

  where $\mathbf{M}^{-1}_{k1,k2}$ denotes the block matrix of $\mathbf{M}^{-1}$ containing the variables of rectangle object k_1 and k_2. The matrices for different k_1 and k_2 overlap, hence the name 'overlapping'. In the overlapping regions all possible contributions according to (13) are summed up.
- WEIGHTED OVERLAPPING BLOCK JACOBI (WOBJAC): Similar to the latter, except $\mathbf{M}^{-1}_{k1,k2}$ is weighted by $\sqrt{n_1 n_2}$, where n_1 and n_2 are numbers of overlaps of the diagonal blocks k_1 and k_2.
- MULTILEVEL (ML): Multilevel preconditioners are successfully used in FEM solvers [13]. Therefore, their application to dense BEM matrices is investigated as well. The hierachical geometric representation in the binary tree is well suited to the multilevel approach which is also related to preconditioners based on Haar wavelets [14]. Consider one cell object k with child objects k_1 and k_2: Let $\mathbf{v}_{kj}$ and $\mathbf{i}_{kj}$ be the area weighted mean of all voltages and currents of all child rectangle objects of k_j ($j = 1$ or 2). One calculation step inside the multilevel preconditioner is

$$\begin{pmatrix} i_{k1} \\ i_{k2} \end{pmatrix} = \begin{pmatrix} Z_{k1} & Z_{k1,k2} \\ Z_{k1,k2} & Z_{k2} \end{pmatrix}^{-1} \begin{pmatrix} v_{k1} \\ v_{k2} \end{pmatrix} \tag{14}$$

  This step is carried out in every cell object. The result i_{k1} and i_{k2} are summed up in every child rectangle.

  The vector $\mathbf{i}$ containing all current variables is the final result of the multilevel preconditioner.

Table 1 presents acceleration results of these preconditioning measures. Computations were carried out on a SunFire 4800 with UltraSparcIII 750 MHz processors and 24 GB memory. It turns out that preconditioning is very important to decrease simulation time. The method 'Weighted Overlapping Block Jacobi' offers the best results. However, its prominence is not very pronounced in this small example, but will be more important for larger problems.

Freq. f	1 Hz		1 MHz		1 GHz	
	It	t	It	t	It	t
Pure BiCG	473	123.2	348	89.7	182	47.5
JAC	38	11.5	38	12.2	38	11.6
BJAC	30	10.1	30	9.5	30	10.1
OBJAC	23	10.7	23	10.9	23	10.7
WOBJAC	21	9.9	21	10.0	20	9.7
ML	27	10.1	30	11.5	33	12.2

Table 1. Number of iterations (It) and runtime (t in seconds) of the CG-algorithm with preconditioners applied to a problem with 8424 variables at different frequencies f.

5. Hierarchical design flow

SUBCALM is implemented as a client-server system. The server program is written in C++ with about 40000 lines of code. PerlTk is used for the GUI. Both parts communicate with each other through TCP/IP or Unix sockets. The software runs under Sun Solaris, Linux or Microsoft Windows. Some additional Perl and SKILL scripts are provided which offer an easy-to-use link to the Cadence design framework DFII.

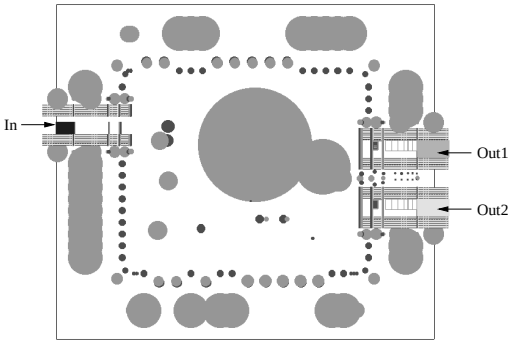

Figure 7. Simulation with macromodels.

A substrate coupling analysis of a photodiode front end amplifier integrated in $0.13\,\mu$m CMOS is presented as an example for the hierarchical SubCALM design flow. It has a single-ended input and a differential output. Due to the high amplification an equivalent circuit describing the coupling from the output to the input had to be found in order to investigate possible instabilities. The floorplan of the chip is

shown in Fig. 7. Simplified macromodels were calculated for every subcircuit. Their circular ports are displayed in Fig. 7. Macromodels with lower abstraction levels or even with the complete original layout were chosen for all the blocks around the input and output bonding pads.

(a)	In	Out1	Out2
VDD	$7.5-94j$	$-155j$	$-156j$
VSS	$76+35j$	$23+1.4j$	$22+1.5j$
In	$134+37j$	$8800+4400j$	$6300+2400j$
Out1		$190+38j$	$420+54j$
Out2			$180+35j$
Number of variables			63196
Macromodel ports			190
Runtime			2970 s

(b)	In	Out1	Out2
VDD	$25-82j$	$34-151j$	$38-152j$
VSS	$82+43j$	$23+1.5j$	$23+1.5j$
In	$142+35j$	$9600+4500j$	$6900+2400j$
Out1		$159+24j$	$440+61j$
Out2			$160+34j$
Number of variables			7280
Macromodel ports			218
Runtime			352 s

Table 2. Simulation results with different macromodel configurations: Simplified macromodels are taken for all subcircuits except (a) subcircuits with input and ouput pads and adjacent ones. (b) subcircuits with input and output pads.

Table 2 presents simulation results for two different macromodel configurations. The given values are coupling impedances between certain electrical nodes, or their self impedance to reference ground, which is either the backplane of the substrate or a floating virtual node at infinity. All values are given in Ω for a frequency of 1 GHz, which is a major working frequency of this chip design example. A BEM-model without precalculated macromodels would consist of about 680000 variables which is impossible to simulate. The simple configuration of Table 2b provides excellent results after only 6 minutes, therefore it is actually not necessary to run the more accurate simulation of Table 2a, since the simulation result of both configurations do not differ very much.

6. Conclusion

A substrate coupling simulation tool named SUBCALM has been developed which offers the opportunity to estimate substrate coupling during floorplanning. It has been shown that acceleration measures like precalculated macromodels reduce the number of variables radically. Furthermore, preconditioning algorithms may be used to decrease the runtime by another order of magnitude. In addition, the new version of SUBCALM also supports triple wells and SOI structures. The possible extension of SUBCALM to capacitance extraction between metal lines will be part of further investigations in the near future.

References

[1] R. Singh, editor. *Signal Integrity Effects in Custom IC and ASIC Design*. Wiley Interscience, 2002.

[2] M. van Heijningen et al. Analysis and experimental verification of digital substrate noise generation for epi-type substrates. *IEEE Journal of Solid-State Circuits*, 35(7):1002–1008, July 2000.

[3] N. K. Verghese, T. J. Schmerbeck, and D. J. Allstot. *Simulation Techniques and Solutions for Mixed-Signal Coupling in Integrated Circuits*. Kluwer Academic Publishers, Boston, 1995.

[4] Cadence, Inc. *SubstrateStorm, www.cadence.com*.

[5] T. Brandtner and R. Weigel. Hierarchical simulation of substrate coupling in mixed-signal ICs considering the power supply network. In *Design Automation and Test in Europe Conference (DATE)*, pages 1028–1032, March 2002.

[6] T. Brandtner and R. Weigel. Simulation and analysis of substrate coupling accelerated by precalculated macromodels. In *Zurich Symposium on Electromagnetic Compatibility (EMC)*, pages 449–454, February 2003.

[7] A. W. Appel. An efficient program for many-body simulation. *SIAM Journal on Scientific and Statistical Computing*, 6(1):85–103, January 1985.

[8] F. Martorell, D. Mateo, and X. Aragones. Modeling and evaluation of substrate noise induced by interconnects. In *Design Automation and Test in Europe Conference (DATE)*, pages 524–529, 2003.

[9] K. Nabors and J. K. White. FastCap: A multipole accelerated 3-D capacitance extraction program. *IEEE Transactions on Computer-Aided Design*, 10(11):1447–1459, November 1991.

[10] W. Shi, J. Liu, N. Kakani, and T. Yu. A fast hierarchical algorithm for three-dimensional capacitance extraction. *IEEE Transactions on Computer-Aided Design of Integrated Circuits and Systems*, 21(3):330–336, March 2002.

[11] R. W. Freund. Conjugate gradient-type methods for linear systems with complex symmetric coefficient matrices. *SIAM Journal on Scientific and Statistical Computing*, 13(1):425–448, January 1992.

[12] Y. Saad. *Iterative Methods for Sparse Linear Systems*. PWS Publishing Company, Boston, MA, 2 edition, 2000.

[13] C. W. Oosterlee and T. Washio. On the use of multigrid as a preconditioner. In *International Conference on Domain Decomposition Methods*, pages 442–448, 1996.

[14] N. Soveiko and M. S. Nakhla. Efficient capacitance extraction computations in wavelet domain. *IEEE Transactions on Circuits and Systems - I: Fundamental Theory and Applications*, 47(5):684–701, May 2000.